Spectral and spatial full-bandwidth correlation analysis of bulk-generated supercontinuum in the mid-infrared

Aymeric van de Walle,[1,2,*] Marc Hanna,[1] Florent Guichard,[1,3] Yoann Zaouter,[3] Alexandre Thai,[2] Nicolas Forget,[2] and Patrick Georges[1]

[1]*Laboratoire Charles Fabry, UMR 8501, Institut d'Optique, CNRS, Univ Paris Sud 11, 2 Av. A. Fresnel, 91127 Palaiseau, France*

[2]*Fastlite, 1900 route des Crêtes 06560 Valbonne, Sophia Antipolis, France*

[3]*Amplitude Systemes, 11 avenue de Canteranne, Cité de la Photonique, 33600 Pessac, France*

**Corresponding author: aymeric.van-de-walle@institutoptique.fr*

We report the measurement of spectral and spatial correlations in supercontinua generated by focusing microjoule pulses from a femtosecond ytterbium-doped fiber amplifier laser in bulk YAG. The measurement is full-bandwidth at a repetition rate of 1 MHz owing to the use of time-stretch dispersive Fourier transform technique. In contrast with fiber-based supercontinuum generation, our results show an excellent stability of the spectral and spatial properties of the output supercontinuum, with an essentially correlated behavior in the 1.4–1.7 μm wavelength range. These results provide strong ground for the development of supercontinuum-seeded ultrafast optical parametric amplifier systems in the mid-infrared using ytterbium lasers as pump sources.

OCIS codes: (320.6629) Supercontinuum generation; (320.7090) Ultrafast lasers; (320.7110) Ultrafast nonlinear optics; (140.3070) Infrared and far-infrared lasers.

Supercontinuum (SC) generation is an extremely nonlinear phenomenon used to generate optical spectra that can extend over several octaves. First reported in bulk media in 1970 [1], it was later observed and studied in optical fibers, where the required power level is much lower. This has enabled SC generation in all temporal regimes, from CW to femtosecond, and triggered numerous applications [2]. The very rich physics of SC generation has been a widely studied subject, both in bulk media [3] and in fibers [2], including recent studies on single-shot characterization [4] and shot-to-shot correlation properties of SC [5–7]. These studies have mostly focused on fiber-generated SCs, since it has been shown that coherence can be quickly lost in this case.

On the other hand, there is an increasing interest for bulk-generated SC to be used as a seed for broadband optical parametric amplification (OPA) systems [8]. In particular, robust high-power ytterbium-based amplified femtosecond laser systems delivering pulses with a duration in a range of 300 fs–1 ps can be used both as a pump source for the OPA system and for the SC generation [9], thereby providing optical synchronization between signal and pump. This is increasingly important in systems where the stretched pulse duration is in the range of 300 fs–10 ps, which are more sensitive to relative timing fluctuations. Bulk SC-seeded OPAs at 800 nm have been extensively studied [10], but are less common in the mid-infrared, despite a large interest in this wavelength range for molecular multidimensional spectroscopy and attophysics applications [11,12]. Although it is known that by operating in the single filament regime, a stable SC beam can be generated in bulk media, there are few reported studies of bulk SC spectral fluctuations and correlations to the best of our knowledge [13,14]. These works focus on the visible part of the SC generated by a Ti:Sa laser in bulk CaF_2 or YAG at low repetition rate. However, the spatial correlation properties have not been investigated yet, a legitimate concern for bulk SCs. Since they are being considered for use as a seed for large OPA-based laser facilities, the question of their spectral and spatial fluctuation dynamics is particularly important.

In this Letter, we report on the full bandwidth spectral and spatial correlation analysis of a mid-infrared SC generated by focusing microjoule femtosecond pulses from a high-energy ytterbium-doped fiber amplifier in bulk YAG. Shot-to-shot measurements at a repetition rate of 1 MHz are obtained by implementing the time-stretch dispersive Fourier transform in an optical fiber to map the spectral domain to the time domain, a technique used in the context of fiber SCs [5–7]. A fast real-time oscilloscope is used to retrieve the temporal data for each shot. Spatial correlations are measured by sampling two copies of the beam at different locations. The results show the overall stability of single-filament bulk SCs, and a correlated noise behavior in the 1.4–1.7 μm wavelength range. The spatial fluctuations are also correlated, and a good spectral homogeneity is observed. Finally, a long-term multi-shot spectral measurement reveals excellent stability over hours. These results support the strong interest of Yb laser-pumped SC-seeded OPA systems in the mid-infrared.

The experimental setup is described in Fig. 1. A half-wave plate and a polarizer are used to sample a pulse energy of 1.8 μJ from an ytterbium-doped rod-type fiber amplifier (Tangerine, Amplitude Systemes). This laser system delivers 400 fs pulses at 1030 nm, with an optical bandwidth of 6 nm at a repetition rate of 1 MHz. The 1.5 mm diameter beam (FWHM) is focused in a 10 mm long YAG crystal with a 125 mm focal length lens to generate the single filament SC. Loose focusing is known to increase the spectral content in the near-infrared [15]. The SC is collimated by another 125 mm lens, filtered to remove the 1 μm pump and isolate the bandwidth

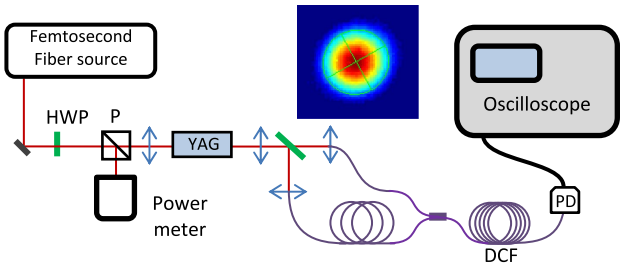

Fig. 1. Experimental setup and spatial profile of the SC mid-IR part. HWP, half-wave plate; P, polarizer; DCF, dispersion compensating fiber; PD, photodetector. Inset: spatial profile of the SC recorded with an InGaAs camera after a 1400 nm longpass filter.

of interest, and split into two beams using a broadband beamsplitter. Each beam is focused down to a diameter of 150 μm (FWHM), where standard SMF28 fibers are located. The difference between the diameter of the focused beam and the 9 μm diameter of the fiber allows spatially selective coupling in the fibers, and scanning the fiber position gives access to spectral measurements that are spatially resolved in the near field. For spatial correlation measurements, both fibers are then coupled to a single fiber using a standard broadband fiber coupler, with a relative delay of 25 ns corresponding to a 5 m fiber additional path length difference. This signal is sent to 260 m of dispersion compensating fiber that introduces a large amount of dispersion to perform the time stretch Fourier transform. A fast InGaAs photodetector and oscilloscope, with overall bandwidth of 8 GHz, allow detection of the stretched pulses. The RMS value of the detection noise is evaluated to be 0.4% of the full detected scale. A single detection fiber is used to measure the spectral correlation properties, and to measure the spectral homogeneity of the beam by scanning the fiber. Both detection fibers are used to compute spatial correlations, since they allow observation of the same train of pulses at two different locations in the beam. Finally, the 1 μm pump is detected independently to measure energy fluctuations of the SC excitation, with a typical value of 1% RMS.

The use of the time-stretch dispersive Fourier transform requires a calibration to map the measured time trace to the spectrum. This is achieved by identifying distinct spectral features and comparing the time signal with an independently measured spectrum from an optical spectrum analyzer. The group-delay introduced by the fiber as a function of wavelength is shown in Fig. 2, with calibration points and a polynomial fit. The oscilloscope-retrieved spectrum using this calibration is shown against an independently measured optical spectrum in the inset. The 1.4–1.7 μm wavelength range is mapped to a 4 ns time window. Taking into account the bandwidth of the detection system, this corresponds to a spectral resolution of 10 nm in this range.

We first examine spectral correlations of the SC by positioning one fiber at the center of the beam, while the other fiber is not used. A data set of 500 successive pulses is acquired and processed. The spectral correlation between two wavelengths, λ_1 and λ_2, in the SC is defined as in Ref. [5], equivalent to the Pearson correlation in Ref. [13]:

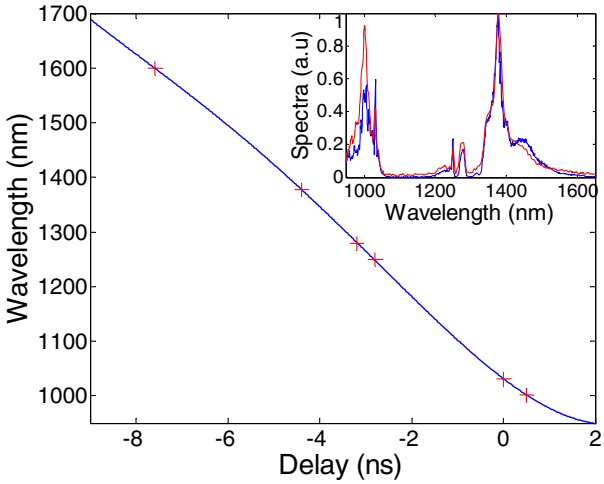

Fig. 2. Calibration curve of the time stretch Fourier transform. Red points are experimental pairs of delay/wavelength, while the blue line is a polynomial fit. Inset: comparison between oscilloscope-retrieved spectrum and independently measured optical spectrum.

$$\rho(\lambda_1,\lambda_2)=\frac{\langle I(\lambda_1)\cdot I(\lambda_2)\rangle-\langle I(\lambda_1)\rangle\cdot\langle I(\lambda_2)\rangle}{\sqrt{(\langle I^2(\lambda_1)\rangle-\langle I(\lambda_1)\rangle^2)\cdot(\langle I^2(\lambda_2)\rangle-\langle I(\lambda_2)\rangle^2)}}. \tag{1}$$

For comparison purpose, the YAG crystal and filter can be removed to generate a fiber SC in the first few meters of SMF28 fiber. The resulting correlation map, along with the accumulated spectra, is shown in Fig. 3. As in previous works on fiber SCs, large spectral instabilities are observed (13.8% RMS near the generation wavelength) with correlation maps similar to previous observations [7]. The correlation is low in the mid infrared, and a feature distinctive of wavelength jitter is observed around the pump wavelength.

In contrast, bulk SC data obtained when a dichroic mirror is used to attenuate the 1 μm pump is shown in Fig. 4. Pump filtering ensures that the highly dispersive fiber does not induce significant nonlinear effects after bulk SC generation. The transmission of the dichroic mirror is not flat over the investigated wavelength range, but this

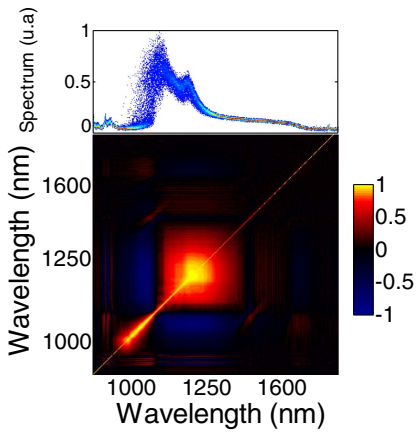

Fig. 3. Results for fiber SC generation. Top: accumulated retrieved spectra. Bottom: spectral correlation map according to Eq. (1).

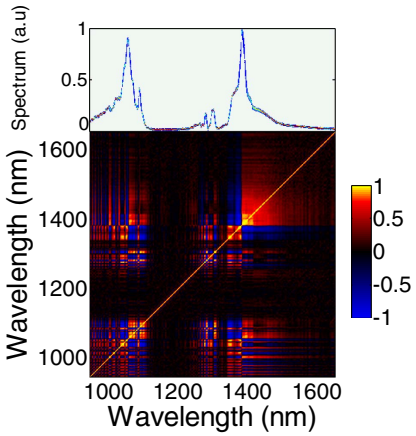

Fig. 4. Results for bulk SC generation. Top: accumulated retrieved spectra. Bottom: spectral correlation map according to Eq. (1).

does not affect the statistical properties of the SC. The most obvious difference with the fiber case is the high stability of spectral features. Although the magnitude of the correlation is always high, illustrating the coherence of the bulk SC process, two spectral ranges exhibiting different qualitative features are observed: (1) rapid alternate correlation and anti-correlation areas for low wavelengths closer to the pump, and (2) a large area where the correlation is large and positive at wavelengths above 1.4 μm. A similar behavior has been observed in the visible range of an SC generated from a Ti:Sa laser at 800 nm [13].

By replacing the dichroic mirror with a long-pass filter at 1.4 μm, we observe specifically the large correlated wavelength band in the near infrared with a better signal-to-noise ratio and wavelength fidelity as shown in Fig. 5. This band is of particular interest for ytterbium systems-pumped mid-IR OPA systems, since it allows the generation of an amplified signal around 1.55 μm, corresponding to a carrier-phase envelope stable idler at 3 μm. The smooth generated spectrum is fully correlated, indicating that the spectrum shape does not fluctuate. The decrease of the correlation value beyond 1500 nm is most probably because of the fact that uncorrelated

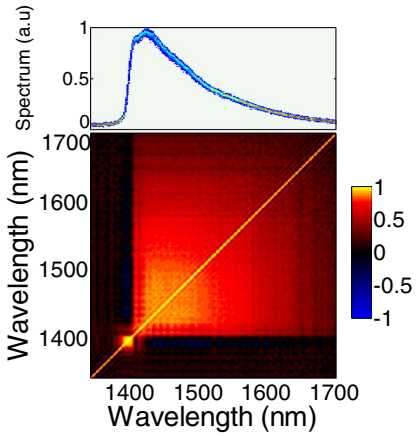

Fig. 5. Results for bulk SC generation in the 1.4–1.7 μm wavelength range. Top: accumulated retrieved spectra. Bottom: spectral correlation map according to Eq. (1).

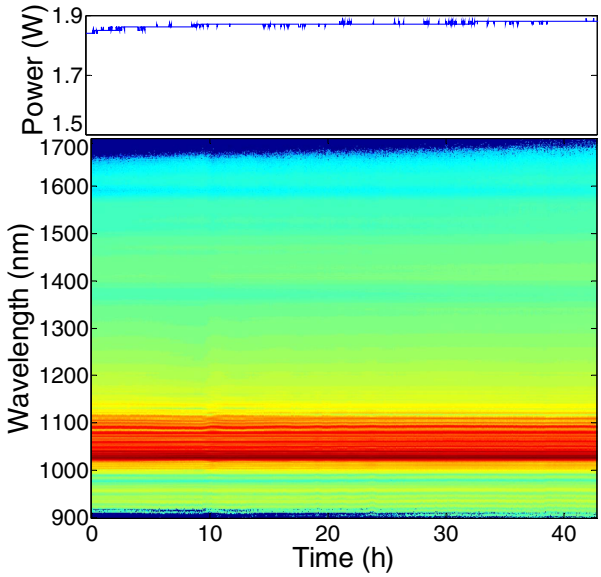

Fig. 6. Top: average pump power as a function of time. Bottom: SC spectrum recorded with an optical spectrum analyzer (log scale) as a function of time over 40 h.

detection noise becomes nonnegligible compared to the signal. To quantify the stability of this signal, the RMS shot-to-shot relative intensity noise of the spectral component at 1550 nm over 500 pulses is 3.4%, compared to 1.2% for the pump intensity noise. This value is particularly important for seeding applications since it impacts the final laser stability.

Long term stability is also a major concern in OPCPA systems. In particular, since SC is generated at intensity levels close to crystal breakdown, slow alteration of the crystalline matrix can occur. The spectrum of the SC is recorded for 40 h to monitor possible spectral drifts, along with the average power of the pump laser. As shown in Fig. 6, the SC spectrum is very stable, except for a slight broadening because of the slow increase of pump power.

We now investigate spatial properties of the SC in the 1.4–1.7 μm range. Since complex spatiotemporal dynamics is involved in bulk SC generation, including filamentation, the question of spectrospatial couplings in the SC beam is natural. Color rings can be routinely observed in such beams [3], indicating large spatial inhomogeneities in the visible region. By translating the collecting fiber in the SC beam (shown in the inset of Fig. 1 as recorded using an InGaAs camera), the mid-infrared spectrum is retrieved as a function of radial coordinate using a standard spectrum analyzer. The power in each retrieved spectrum is normalized to remove the decrease in intensity because of lateral displacement, and this data is plotted in Fig. 7. The spectral homogeneity in this band is remarkably good, with only a slightly larger extension toward the long wavelength side for the outer part of the beam.

By using both collecting fibers, we can measure spatial correlations in the beam to track potential fluctuations of the beam shape at the shot-to-shot level. The spatial correlation between two positions, x_1 and x_2, at a given wavelength λ is given by

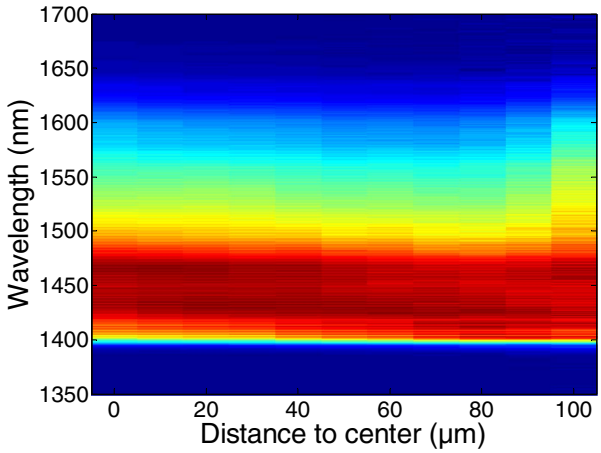

Fig. 7. Normalized SC spectrum as a function of radial coordinate across the beam.

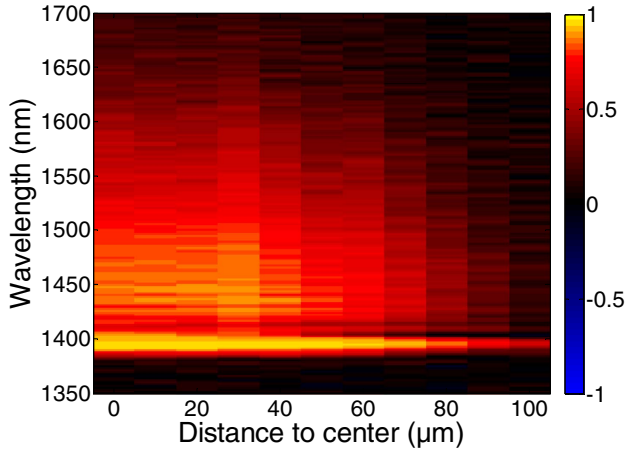

Fig. 8. Spatial correlation map with the center of the beam as a function of the radial coordinate and wavelength.

$$\rho(x_1, x_2, \lambda) = \frac{\langle I(x_1,\lambda)\cdot I(x_2,\lambda)\rangle - \langle I(x_1,\lambda)\rangle\cdot\langle I(x_2,\lambda)\rangle}{\sqrt{(\langle I^2(x_1,\lambda)\rangle - \langle I(x_1,\lambda)\rangle^2)\cdot(\langle I^2(x_2,\lambda)\rangle - \langle I(x_2,\lambda)\rangle^2)}}. \quad (2)$$

The correlation map between the center of the beam ($x_1 = 0$) and the beam sampled at a given radial coordinate as a function of wavelength is plotted in Fig. 8. The wavelength correlation map shows a fully correlated behavior of the mid infrared beam. The decrease of the correlation coefficient at long wavelengths is because of the limited signal to noise ratio: uncorrelated detection noise is not negligible in this case and decreases the correlation coefficient.

In conclusion, we have studied spectral and spatial statistical properties of bulk SC generated by focusing 1.8 μJ 400 fs pulses at the wavelength of 1030 nm in bulk YAG. The stability and correlation properties of this radiation in the near infrared wavelengths between 1.4 and 1.7 μm are remarkably good, with only a minor degradation of RMS relative noise intensity compared to the pump. The spatial homogeneity and correlations are also well behaved, advocating the use of these SCs as seed beams for near-infrared ultrafast OPAs.

This work was supported by the FUI project STAR and LABEX PALM project MIROPCPA.

References

1. R. R. Alfano and S. L. Shapiro, Phys. Rev. Lett. **24**, 584 (1970).
2. J. M. Dudley, G. Genty, and S. Coen, Rev. Mod. Phys. **78**, 1135 (2006).
3. A. Couairon and A. Mysyrowicz, Phys. Rep. **441**, 47 (2007).
4. T. C. Wong, M. Rhodes, and R. Trebino, Optica **1**, 119 (2014).
5. B. Wetzel, A. Stefani, L. Larger, P.-A. Lacourt, J.-M. Merolla, T. Sylvestre, A. Kudlinski, A. Mussot, G. Genty, F. Dias, and J. M. Dudley, Sci. Rep. **2**, 882 (2012).
6. T. Godin, B. Wetzel, T. Sylvestre, L. Larger, A. Kudlinski, A. Mussot, A. Ben Salem, M. Zghal, G. Genty, F. Dias, and J. M. Dudley, Opt. Express **21**, 18452 (2013).
7. Z. Ren, Y. Xu, Y. Qiu, K. Y. Wong, and K. Tsia, Opt. Express **22**, 11849 (2014).
8. M. K. Reed, M. K. Steiner-Shepard, and D. K. Negus, Opt. Lett. **19**, 1855 (1994).
9. M. Bradler, P. Baum, and E. Riedle, Appl. Phys. B **97**, 561 (2009)
10. G. Cerullo and S. De Silvestri, Rev. Sci. Instrum. **74**, 1 (2003).
11. A. Thai, M. Hemmer, P. K. Bates, O. Chalus, and J. Biegert, Opt. Lett. **36**, 3918 (2011).
12. B. W. Mayer, C. R. Phillips, L. Gallmann, M. M. Fejer, and U. Keller, Opt. Lett. **38**, 4265 (2013).
13. M. Bradler and E. Riedle, J. Opt. Soc. Am. B **31**, 1465 (2014).
14. D. Majus and A. Dubietis, J. Opt. Soc. Am. B **30**, 994 (2013).
15. V. Jukna, J. Galinis, G. Tamosauskas, D. Majus, and A. Dubietis, Appl. Phys. B **116**, 477 (2014).